Targeted energy transfer with parallel nonlinear energy sinks. Part I: Design theory and numerical results

Bastien Vaurigaud, Alireza Ture Savadkoohi, Claude-Henri Lamarque

Abstract In this paper, we study a Targeted Energy Transfer (TET) problem between a p degrees-of-freedom (dof) linear master structure and several coupled parallel slave Nonlinear Energy Sink (NES) systems. In detail, each lth dof $l = 1, 2, \ldots, p$ contains n_l parallel NES; so the linear structure has $(n_1 + n_2 + \cdots + n_l + \cdots + n_p)$ NES. We are interested to study analytically the TET phenomenon during the first mode of the compound system. To this end, complexification, averaging, and multiple scales methods are used.

The system is studied under 1:1 resonance for the transient regime and under harmonic excitation. The influence of the system parameters is observed through dimensionless variables. An analytical criterion is defined to tune NES parameters which lead to an efficient TET for the transient and the forced regimes. It will be demonstrated that analytical results are in good agreement with numerical ones.

This paper will be followed by a companion paper which mainly deals with the governing equations for compound nonlinear systems with trees of NES devices at each dof; then experimental results of a four storey structure with two parallel NES at the top floor which are tuned by the mentioned technique in the current paper will be demonstrated and commented upon.

Keywords Transient regime · Stationary regime · Complexification · Multiple scales · Bifurcations · Tuning · NES in parallel

Nomenclature

$c_{n,j}$	damping of NES j attached to the dof n
$k_{n,j}$	stiffness of NES j attached to the dof n
q_1	first mode generalized displacement of the linear system
$x_{n,j}$	displacement of NES j attached to the dof n
C_1^*	first mode modal damping of the linear system
$F_n(t)$	external forcing on dof n
K_1^*	first mode modal stiffness of the linear system
M_1^*	first mode modal mass of the linear system
$\phi_{n,1}$	first mode modal shape of the linear system at dof n

1 Introduction

A numerous number of seismic mitigation devices has been developed during the past decades [1]. Novel designs of structures commonly seek to reduce the total structural mass. Thus, it is important to develop new absorption devices that reduce both stationary and transient responses as much as possible while adding as less as possible extra mass to the structure; moreover these devices should be able to absorb seismic effects for a broadband of frequencies. To this end, NES

B. Vaurigaud (✉) · A. Ture Savadkoohi · C.-H. Lamarque
Université de Lyon, ENTPE/DGCB/FRE CNRS 3237,
3 rue Maurice Audin, 69518, Vaulx-en-Velin Cedex,
France
e-mail: bastien.vaurigaud@entpe.fr

systems have been developed that the imposed energy to a linear single dof system is transferred to a strongly nonlinear light attachment in an irreversible manner; the mechanism is mainly based on a 1:1 resonance capture and involves the Nonlinear Normal Modes geometry. Theoretical background of these systems is quite well developed [2–13]. The overall system behavior during the energy absorption by nonlinear absorbers is based on complete detection of nonlinear normal modes (NNM) of the system. The reader can refer to [14] for detailed information about NNM and localization. Manevitch et al. [11, 15] presented new analytical approach to the problem of energy pumping in strongly nonhomogeneous nonlinear two dof systems with single anchor spring under impulse load due to initial conditions. Their approach was based on application of the equations of motion in complex form and using the power expansion of the solution in terms of time. Schmidt and Lamarque [16] studied the energy transfer from initial single dof system including nonsmooth term of friction to a NES under free transient or periodic external excitations. They illustrated that under free excitation, a NES tuned for underlying linear elastic oscillator is still efficient for the elastoplastic case and leads to reduce oscillations in comparison with the behavior without coupled NES. They showed that under periodic excitation and the same design, efficiency of energy pumping can be reduced or destroyed in the whole system, but it is possible to improve the design by a numerical parametric study to get correct results. Manevitch and Manevitch [17] presented an analytical and numerical study of the energy exchange and transfer in a strongly nonlinear two dof system subject to resonance 1:1 based on the concept of the Limiting Phase Trajectories (LPTs). Their approach allowed constructing an approximate analytic solution describing the energy exchange and beating with complete energy transfer in the system. Pham et al. [18] analyzed combination resonance for a two degrees-of-freedom system that consists of one master system involving the main basic quadratic nonlinearity and one NES with purely cubic nonlinear term. The idea of the relative mode was endowed for proving the efficiency of the NES in controlling the system.

McFarland et al. [19] and Gourdon et al. [20, 21] experimentally verified theoretical effects of energy pumping with a single NES coupled with single and four dof systems, respectively. They experimentally proved the efficiency of energy pumping systems with respect to classical tuned mass dampers. All of above mentioned analytical and experimental researches were carried out on structures with single NES devices. In the current and companion papers, we will present analytical and experimental studies about compound nonlinear systems with parallel NES devices, respectively.

The outline of the paper is as follows. Section 2 presents the reduced equations of the compound system. In Sect. 3, analytical and numerical studies are presented for the transient behavior of the system and an analytical triggering criterion for TET is defined. In Sect. 4, these investigations are extended to the forced case under harmonic excitation. Finally, conclusions are given in Sect. 5.

2 Dynamics of the system

We investigate the case of a p dof linear master structure which is coupled to $(n_1 + n_2 + \cdots + n_p)$ cubic NES. The $\mathrm{NES}_{n,j}$ is the jth NES that is coupled to degree of freedom n. All of $\mathrm{NES}_{n,j}$ are parallel with each other. This nonlinear coupling aims at controlling the first mode of this p dof structure by determining efficient physical parameters for the different NES. We will shift from physical domain to the modal domain by appropriate change of variables. To design different NES, we first reduce the linear system to its first mode (the one to be controlled), and then we observe the coupling between this mode and the $(n_1 + n_2 + \cdots + n_p)$ NES. These assumptions lead to the following system of equations:

$$\begin{cases} M_1^* \ddot{q}_1 + C_1^* \dot{q}_1 + K_1^* q_1 + \displaystyle\sum_{l=1}^{p} \sum_{j=1}^{n_l} \phi_{l,1} \mu_{l,j} \ddot{x}_{l,j} \\ \quad = \displaystyle\sum_{l=1}^{p} \phi_{l,1} F_l(t) \\ \quad \forall n = 1..p,\ \forall j = 1..n_n \\ \mu_{n,j} \ddot{x}_{n,j} + c_{n,j}(\dot{x}_{n,j} - \phi_{n,1} \dot{q}_1) \\ \quad + k_{n,j}(x_{n,j} - \phi_{n,1} q_1)^3 = 0. \end{cases} \tag{1}$$

where n_n is the number of attached parallel NES to the dof n. The different parameters and variables are defined in the nomenclature.

3 Transient behavior under impulse load

In this section, we study the transient behavior of the coupled system which is reduced to a single mode in the vicinity of 1:1 resonance. Analytical approximation of the response using dimensionless variables are obtained and a tuning procedure for the NES is established. Numerical simulations are performed for the case of two NES in parallel which are attached to the same dof.

Under this assumption, (1) can be rewritten as

$$\begin{cases} M_1^*\ddot{q}_1 + C_1^*\dot{q}_1 + K_1^* q_1 + \sum_{l=1}^{p}\sum_{j=1}^{n_l}\phi_{l,1}\mu_{l,j}\ddot{x}_{l,j} = 0 \\ \quad \forall n = 1..p,\ \forall j = 1..n_n \\ \mu_{n,j}\ddot{x}_{n,j} + c_{n,j}(\dot{x}_{n,j} - \phi_{n,1}\dot{q}_1) \\ \quad + k_{n,j}(x_{n,j} - \phi_{n,1}q_1)^3 = 0 \end{cases} \tag{2}$$

Let us consider the system without external forcing with the following initial conditions:

$$\begin{cases} q_1(0) = 0, \qquad \dot{q}_1(0) \neq 0 \\ x_{n,j}(0) = 0, \qquad \forall n = 1..p,\ \forall j = 1..n_n \end{cases} \tag{3}$$

Now, let us introduce following change of variables:

$$\begin{cases} \dfrac{\mu_{n,j}}{M_1^*} = \varepsilon\alpha_{n,j}, \qquad \displaystyle\sum_{n=1}^{p}\sum_{j=1}^{n_l}\alpha_{n,j} = 1 \\ \dfrac{c_{n,j}}{M_1^*} = \varepsilon\alpha_{n,j}\lambda_{n,j}, \qquad \dfrac{k_{n,j}}{M_1^*} = \varepsilon\alpha_{n,j}\Omega_{n,j}\omega_0^{*4} \\ \dfrac{C_1^*}{M_1^*} = \varepsilon\lambda^*, \qquad \dfrac{K_1^*}{M_1^*} = \omega_0^{*2} \end{cases} \tag{4}$$

Then (2) will read as

$$\begin{cases} \ddot{q}_1 + \varepsilon\lambda^*\dot{q}_1 + \omega_0^{*2}q_1 + \varepsilon\displaystyle\sum_{l=1}^{p}\sum_{j=1}^{n_l}\phi_{l,1}\alpha_{l,j}\ddot{x}_{l,j} = 0 \\ \quad \forall n = 1..p,\ \forall j = 1..n_n \\ \varepsilon\alpha_{n,j}\ddot{x}_{n,j} + \varepsilon\alpha_{n,j}\lambda_{n,j}(\dot{x}_{n,j} - \phi_{n,1}\dot{q}_1) \\ \quad + \varepsilon\alpha_{n,j}\Omega_{n,j}\omega_0^{*4}(x_{n,j} - \phi_{n,1}q_1)^3 = 0 \end{cases} \tag{5}$$

New variables are introduced, which are in fact center of mass u and internal displacements $v_{n,j}$:

$$\begin{cases} u = q_1 + \varepsilon\displaystyle\sum_{l=1}^{p}\sum_{j=1}^{n_l}\phi_{l,1}\alpha_{l,j}x_{l,j} \\ v_{n,j} = x_{n,j} - \phi_{n,1}q_1, \quad \forall n = 1..p, \forall j = 1..n_n \end{cases} \tag{6}$$

which reduce (5) to the following form:

$$\begin{aligned} &\ddot{u} + \varepsilon\lambda^*\frac{\dot{u} + \varepsilon\sum_{l=1}^{p}\sum_{j=1}^{n_l}\alpha_{n,j}\phi_{l,1}\dot{v}_{n,j}}{1+\varepsilon Y} \\ &\quad + \omega_0^{*2}\frac{u + \varepsilon\sum_{l=1}^{p}\sum_{j=1}^{n_l}\alpha_{n,j}\phi_{n,j}v_{n,j}}{1+\varepsilon Y} = 0 \end{aligned} \tag{7}$$

$$\begin{aligned} &\varepsilon\ddot{v}_{n,j} + \varepsilon\phi_{n,j}\frac{\ddot{u} + \varepsilon\sum_{l=1}^{p}\sum_{j=1}^{n_l}\alpha_{n,j}\phi_{n,j}\ddot{v}_{n,j}}{1+\varepsilon Y} \\ &\quad + \varepsilon\lambda_{n,j}v_{n,j} + \varepsilon\Omega_{n,j}\omega_0^{*4}v_{n,j}^3 = 0, \\ &\quad \forall n = 1..p,\ \forall j = 1..n_n \end{aligned} \tag{8}$$

with $Y = \sum_{l=1}^{p}\sum_{j=1}^{n_l}\phi_{l,1}^2\alpha_{n,j}$.

We are investigating the first order approximation of the solution in the vicinity of 1:1 resonance. We introduce this 1:1 resonance in (8). Then we conserve only terms until order ε^1 in (7), and (8):

$$\begin{aligned} &\left(\ddot{u} + \omega_0^{*2}u\right) + \varepsilon\left[\lambda^*\dot{u} + \omega_0^{*2}\sum_{l=1}^{p}\sum_{j=1}^{n_l}\alpha_{n,j}\phi_{n,j}v_{n,j}\right] \\ &\quad - \varepsilon\left[\omega_0^{*2}\sum_{l=1}^{p}\sum_{j=1}^{n_l}\alpha_{n,j}\phi_{n,j}^2 u\right] + o(\varepsilon^2) = 0 \end{aligned} \tag{9}$$

$$\begin{aligned} &\varepsilon\left(\ddot{v}_{n,j} + \omega_0^{*2}v_{n,j}\right) + \varepsilon\phi_{n,j}\omega_0^{*2}u + \varepsilon\lambda_{n,j}\dot{v}_{n,j} \\ &\quad + \varepsilon\Omega_{n,j}\omega_0^{*4}v_{n,j}^3 \\ &\quad - \varepsilon\omega_0^{*2}v_{n,j} + o\left(\varepsilon^2\right) = 0, \\ &\quad \forall n = 1..p,\ \forall j = 1..n_n \end{aligned} \tag{10}$$

Complex variables of Manevitch [22] and multiple scales expansions [23] are introduced in (9) and (10) according to the following relations:

$$\begin{aligned} &\varphi_0 e^{i\omega_0^* t} = \dot{u} + i\omega_0^* u \\ &\varphi_{n,j}e^{i\omega_0^* t} = \dot{v}_{n,j} + i\omega_0^* v_{n,j} \\ &\quad \forall n = 1..p,\ \forall j = 1..n_n, \\ &\varphi_0 = \varphi_{00} + \epsilon\varphi_{01} + \epsilon^2\varphi_{02} + \cdots \\ &\quad \forall n = 1..p,\ \forall j = 1..n_n, \\ &\varphi_{n,j} = \varphi_{nj0} + \epsilon\varphi_{nj1} + \epsilon^2\varphi_{nj2} + \cdots \\ &\quad \text{for } l = 0, 1, 2, \ldots\ T_l = \varepsilon^l t, \\ &\frac{d}{dt} = \frac{\partial}{\partial T_0} + \varepsilon\frac{\partial}{\partial T_1} + \varepsilon^2\frac{\partial}{\partial T_2} + \cdots. \end{aligned} \tag{11}$$

By considering secular terms relevant to $e^{i\omega_0^* t}$ in the resulting equation we obtain:

- Order ε^0 of (9):

$$\frac{\partial \varphi_{00}}{\partial T_0} = 0 \tag{12}$$

- Order ε^1 of (9):

$$\frac{1}{\omega_0^*}\frac{\partial \varphi_{00}}{\partial T_1} = \frac{-\zeta^*}{2}\varphi_{00} - \frac{i}{2}\sum_{l=1}^{p}\sum_{j=1}^{n_l}\alpha_{n,j}\phi_{n,j}^2\varphi_{00} + \frac{i}{2}\sum_{l=1}^{p}\sum_{j=1}^{n_l}\alpha_{n,j}\phi_{n,j}\varphi_{nj0} \tag{13}$$

- Order ε^1 of (10):

$$\frac{1}{\omega_0^*}\frac{\partial \varphi_{nj0}}{\partial T_0} = \frac{i}{2}\phi_{nj}\varphi_{00} - \frac{(i+\zeta_{n,j})}{2}\varphi_{nj0} + \frac{3i\Omega_{n,j}}{8}|\varphi_{nj0}|^2\varphi_{nj0} \quad \forall n = 1..p,\ \forall j = 1..n_n \tag{14}$$

where $\zeta^* = \frac{\lambda^*}{\omega_0^*}$ and $\zeta_{n,j} = \frac{\lambda_{n,j}}{\omega_0^*}$.

It can be demonstrated that variables φ_{nj0} evolve toward an equilibrium state [6] such as

$$\begin{cases} \forall n = 1..p,\ \forall j = 1..n_n, \\ \dfrac{i}{2}\phi_{n,j}\varphi_{00} - \dfrac{(i+\zeta_{n,j})}{2}\Phi_{nj0} + \dfrac{3i\Omega_{n,j}}{8}|\Phi_{nj0}|^2\Phi_{nj0} \\ \quad = 0, \\ \Phi_{nj0}(T_1,\ldots) = \lim\limits_{T_0\to\infty}\varphi_{nj0}(T_0,T_1,\ldots) \end{cases} \tag{15}$$

By rewriting complex variables in polar form:

$$\begin{cases} \varphi_{00} = R_0(T_1)e^{i\delta_0(T_1)} \\ \Phi_{nj0} = R_{nj}(T_1)e^{i\delta_{n,j}(T_1)} \\ \quad \forall n = 1..p,\ \forall j = 1..n_n \end{cases} \tag{16}$$

Now, (13) and (15) can be rewritten as

$$\begin{cases} \dfrac{1}{\omega_0^*}\dfrac{\partial R_0^2}{\partial T_1} = -\zeta^* R_0^2 - \sum\limits_{l=1}^{p}\sum\limits_{j=1}^{n_l}\alpha_{n,j}\zeta_{n,j}R_{nj}^2 \\ \phi_{n,j}^2 R_0^2 = \left[\zeta_{n,j}^2 + \left(1 - \dfrac{3\Omega_{n,j}}{4}R_{nj}^2\right)^2\right]R_{nj}^2 \\ \quad \forall n = 1..p,\ \forall j = 1..n_n \end{cases} \tag{17}$$

Let us assume that $E_{nj} = \Omega_{n,j}R_{nj}^2$ and $E_0 = \Omega_{n,j}R_0^2$, then (17) read as

$$\frac{\partial E_0}{\partial T_1} = -\lambda^* E_0 - \sum_{l=1}^{p}\sum_{j=1}^{n_l}\alpha_{n,j}\lambda_{n,j}E_{nj} \tag{18}$$

$$\phi_{n,j}^2 E_0 = \left[\zeta_{n,j}^2 + \left(1 - \frac{3}{4}E_{nj}\right)^2\right]E_{nj} \quad \forall n = 1..p,\ \forall j = 1..n_n \tag{19}$$

where E_0 and E_{nj} are dimensionless variables which depend on initial conditions and the nonlinearity of the system.

$$\begin{cases} E_0 = \Omega_{n,j}|\varphi_{00}|^2 = \Omega_{n,j}\left(\dot{u}_0^2 + \omega_0^{*2}u_0^2\right) \\ \quad \forall n = 1..p,\ \forall j = 1..n_n, \\ E_{nj} = \Omega_{n,j}|\Phi_{nj0}|^2 \\ \quad = \Omega_{n,j}\left(\lim\limits_{T_0\to\infty}\left[\dot{v}_{nj0}^2 + \omega_0^{*2}v_{nj0}^2\right]\right) \end{cases} \tag{20}$$

Variables E_0 and E_{nj} are dimensionless variables which represent the behavior of the main linear mode (E_0) and internal nonlinear modes ($E_{nj}, \forall n = 1..p$, $\forall j = 1..n_n$) at each attachment for $T_0 \to \infty$. Equation (19) represents the asymptotic relation between E_0 and E_{nj} at the slow time scale T_1 after suppressing fast oscillations of time scale T_0.

Equation (18) illustrates the mechanism of decreasing oscillation in the main system (E_0). We see that this decrease is controlled by the damping of the master system (λ^*) and additional damping which are generated by NES ($\lambda_{n,j}$).

We can observe that NES in parallel contribute to the energetic decrease proportionally to their damping factor multiplied by their own mass. It is also important to denote that these different and independent NES dissipation factors act additionally. Actually (18) underlines the linear additivity of damping factors of NES in parallel.

Equation (19) shows that the energy of each internal mode only depends on the energy of the main linear mode, i.e., each internal mode acts independently. There is no energy transfer between the different absorbers in the first order approximation. Each NES has its own behavior which depends only on the energy of the main linear system, so that in first order approximation adding an additional NES will not affect the efficiency of other NES systems.

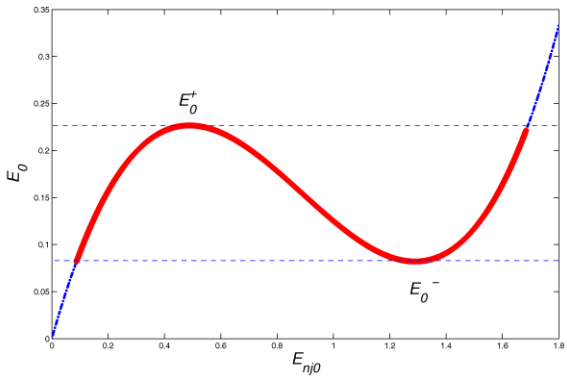

Fig. 1 Multiplicity of solution between dimensionless variables E_0 and E_{nj0}, with $\zeta_{nj} = 0.25$ and $\phi_{nj} = 1$

3.1 Tuning of the NES

The two principles of linear additivity and separated activity of NES in parallel underline that the efficiency of each NES, in the first order approximation, is entirely governed by its own physical parameters, i.e., m_{nj}, c_{nj}, and k_{nj}. This leads us to be able to study the energy activation level for the TET by considering the energy of the master structure sent to each single NES.

Figure 1 shows the multiplicity of solution computed from (19). It has been demonstrated in previous researches [24] that this multiplicity is responsible for the TET. In fact, this bifurcation defines an area where the energy can suddenly jump from high to low levels.

This area of bifurcation can be analytically studied from the derivative of (19):

$$\frac{dE_0}{dE_{nj0}} = \frac{1}{\phi_{n,j}^2}\left[\frac{27}{16}E_{nj0}^2 - 3E_{nj0} + \left(1+\zeta_{n,j}^2\right)\right] \quad (21)$$

If $\zeta_{n,j} \in [0, \frac{1}{\sqrt{3}}]$, then we may obtain multiple solutions for (21). This is a known result in TET. The bifurcation which leads to the energy pumping, due to multiplicity of solutions, only occurs for small values of damping of absorbers [6].

There are two extreme limits in the curve of Fig. 1: E_0^+ and E_0^-, respectively. These coordinates are given by the nullity of derivative of (21).

For the sake of simplicity, we define following functions:

$$\begin{cases} \Delta(\zeta) = 9 - \dfrac{27}{4}(1+\zeta^2) \\ \gamma^+(\zeta) = \dfrac{24 + 8\sqrt{\Delta(\zeta)}}{27}; \\ \gamma^-(\zeta) = \dfrac{24 - 8\sqrt{\Delta(\zeta)}}{27} \end{cases} \quad (22)$$

$$\begin{cases} (E_{nj0}^-; E_0^+) \\ \quad = \left[\gamma^-(\zeta_{n,j});\ \dfrac{1}{\phi_{n,j}^2}\left(\zeta_{n,j}^2 \right.\right. \\ \qquad \left.\left. + \left(1 - \dfrac{3}{4}\gamma^-(\zeta_{n,j})\right)^2\right)\gamma^-(\zeta_{n,j})\right] \\ (E_{nj0}^+; E_0^-) \\ \quad = \left[\gamma^+(\zeta_{n,j});\ \dfrac{1}{\phi_{n,j}^2}\left(\zeta_{n,j}^2 \right.\right. \\ \qquad \left.\left. + \left(1 - \dfrac{3}{4}\gamma^+(\zeta_{n,j})\right)^2\right)\gamma^+(\zeta_{n,j})\right] \end{cases} \quad (23)$$

Different behaviors can be observed along this curve, depending on the initial value of E_0, i.e., the initial energy of the master structure which is activated by its initial conditions. There are several cases as it follows: $E_0 \in [E_0^-, E_0^+]$, $E_0 < E_0^-$ and $E_0 > E_0^+$. Nguyen [25] demonstrated that the most efficient case which leads quickly to a stable and an efficient TET is when $E_0 > E_0^+$.

In this case, the main system crosses the bifurcation and is quickly attracted to the low branch of the curve, which leads to a jump down for the energy of the main system. This jump demonstrates an efficient TET from the main linear system to the considered attachment, and reduces significantly vibrations of the master structure.

This criterion will be endowed to design an efficient NES. As soon as we know the initial condition of the system, i.e., an estimation of the energy E_0 to be controlled, we will be able to evaluate physical parameters of the NES that will immediately trigger the energy pumping and establish an efficient control.

The optimal case for E_0 is to be just above E_0^+, otherwise if E_0 is too high the system will take time to linearly dissipate the energy before reaching the threshold of the TET.

A convenient design for the NES is

$$\begin{cases} E_0 \in [E_0^+, E_0^+ + \chi] \\ E_0^+ = \dfrac{1}{\phi_{n,j}^2}\left(\zeta_{n,j}^2 + \left(1 - \dfrac{3}{4}\gamma^-(\zeta_{n,j})\right)^2\right)\gamma^-(\zeta_{n,j}) \\ \quad \Rightarrow \quad \Omega_{n,j}|\varphi_{00}|^2 \in [E_0^+; E_0^+ + \chi] \end{cases} \tag{24}$$

where χ is a small parameter such as $\chi \ll E_0^+$. We finally obtain the tuning for the stiffness of the NES j which is attached to the dof n of the modal shape $\phi_{n,j}$ as it follows:

$$\begin{cases} k_{n,j} \in [k_{\text{opt}}, k_{\text{opt}} + \chi] \\ k_{\text{opt}} \approx \dfrac{\mu_{n,j}\omega_0^{*4}}{\phi_{n,j}^2|\varphi_{00}|^2}\left(\zeta_{n,j}^2 + \left(1 \right.\right. \\ \qquad \left.\left. - \dfrac{3}{4}\gamma^-(\zeta_{n,j})\right)^2\right)\gamma^-(\zeta_{n,j}) \end{cases} \tag{25}$$

The main results of this analytical study presented in (18), (19), and (25) underline the interest of using parallel NES instead of single NES. Let us consider a NES with mass m, damping c and nonlinear stiffness k_{nl}. This NES can be easily replaced by two NES in parallel of masses $\frac{m}{2}$, damping c; according to (25) to keep the same level of activation these two NES will only require a nonlinear stiffness of $\frac{k_{nl}}{2}$. We notice that the use of parallel NES allows to disseminate the mass along the structure and significantly reduces the required nonlinear stiffness for activation, which could be very interesting for practical applications. Moreover, according to (18), the two NES in parallel will have an equivalent damping of $2c$, which means that this configuration will be more efficient than the corresponding single NES system (the equivalent damping is $2c$, but each NES keeps a damping of c, with c below the critical damping).

Finally, according to the principle of separated activation of (19) the parallel NES configuration can also be interesting to build NES with several levels of activation that could be able to control several modes of a linear structure, by tuning each NES or groups of NES on a chosen linear mode.

3.2 Two NES in parallel

In this subsection, we consider the relevant case of two parallel NES which are attached to the relevant dof of modal shapes $\phi_{n,1}$ and $\phi_{n,2}$. The mass, damping, and stiffness of these NES are $(\mu_{n,1}, \mu_{n,2})$, $(c_{n,1}, c_{n,2})$ and $(k_{n,1}, k_{n,2})$, respectively.

In this case, (2) can be rewritten as

$$\begin{cases} M_1^*\ddot{q}_1 + C_1^*\dot{q}_1 + K_1^*q_1 + \phi_{n,1}\mu_{n,1}\ddot{x}_{n,1} \\ \quad + \phi_{n,2}\mu_{n,2}\ddot{x}_{n,2} = 0 \\ \mu_{n,1}\ddot{x}_{n,1} + c_{n,1}(\dot{x}_{n,1} - \phi_{n,1}\dot{q}_1) \\ \quad + k_{n,1}(x_{n,1} - \phi_{n,1}q_1)^3 = 0 \\ \mu_{n,2}\ddot{x}_{n,2} + c_{n,2}(\dot{x}_{n,2} - \phi_{n,2}\dot{q}_1) \\ \quad + k_{n,2}(x_{n,2} - \phi_{n,2}q_1)^3 = 0 \end{cases} \tag{26}$$

By considering all the change of variables that have been introduced, one can reach the following system of equations:

$$\begin{cases} \dfrac{1}{\omega_0^*}\dfrac{\partial R_0^2}{\partial T_1} = -\zeta^* R_0^2 - \alpha_{n,1}\zeta_{n,1}R_{n1}^2 - \alpha_{n,2}\zeta_{n,2}R_{n2}^2 \\ \phi_{n,1}^2 R_0^2 = \left[\zeta_{n,1}^2 + \left(1 - \dfrac{3\Omega_{n,1}}{4}R_{n1}^2\right)^2\right]R_{n1}^2 \end{cases} \tag{27}$$

After several mathematical manipulations on (27), we obtain the following differential equation that governs the system behavior:

$$\begin{cases} \dfrac{1}{\phi_{n,1}^2\omega_0^*}\dfrac{dR_{n1}^2}{dT_1} \\ \quad = -\dfrac{16}{K}\zeta^* R_0^2 + \dfrac{-16(\alpha_{n,1}\zeta_{n,1}R_{n1}^2 + \alpha_{n,2}\zeta_{n,2}R_{n2}^2)}{K} \\ \quad K = 16\left(1 + \zeta_{n,1}^2\right) - 48\Omega_{n,1}R_{n,1}^2 + 27\Omega_{n,1}^2 R_{n,1}^4 \end{cases} \tag{28}$$

The tuning parameters for each NES can be defined as

$$\begin{cases} k_{n,1}^{\text{opt}} \approx \dfrac{\mu_{n,1}\omega_0^{*4}}{\phi_{n,1}^2|\varphi_{00}|^2}\left(\zeta_{n,1}^2 \right. \\ \quad \left. + \left(1 - \dfrac{3}{4}\gamma^-(\zeta_{n,1})\right)^2\right)\gamma^-(\zeta_{n,1}) \\ k_{n,2}^{\text{opt}} \approx \dfrac{\mu_{n,2}\omega_0^{*4}}{\phi_{n,2}^2|\varphi_{00}|^2}\left(\zeta_{n,2}^2 \right. \\ \quad \left. + \left(1 - \dfrac{3}{4}\gamma^-(\zeta_{n,2})\right)^2\right)\gamma^-(\zeta_{n,2}) \end{cases} \tag{29}$$

Let us consider the case where the two NES have the same modal shape factor $\phi_n = \phi_{n,1} = \phi_{n,2}$. Moreover,

we consider that the design of the two NES leads to the same damping, which means $\zeta_n = \zeta_{n,1} = \zeta_{n,2}$. This configuration of NES is considered for the sake of experimental test set up which will be presented in the companion paper. Even if this case brings a lot of simplifications compared to the considered general case, a similar analytical study could be undertake for p NES disseminated along the structure. To optimize the control process, the two NES are tuned on the same level of activation. According to (29), we have

$$\frac{k_{n,1}}{\mu_{n,1}} = \frac{k_{n,2}}{\mu_{n,2}} \quad \Rightarrow \quad \Omega_n = \Omega_{n,1} = \Omega_{n,2} \tag{30}$$

We reduce (17) to

$$\begin{cases} \phi_n^2 R_0^2 \\ \quad = \left[\zeta_n^2 + \left(1 - \dfrac{3\Omega_n}{4} R_{n1}^2\right)^2\right] R_{n1}^2 \\ \phi_n^2 R_0^2 = \left[\zeta_n^2 + \left(1 - \dfrac{3\Omega_n}{4} R_{n2}^2\right)^2\right] R_{n2}^2 \\ \left[\zeta_n^2 + \left(1 - \dfrac{3\Omega_n}{4} R_{n1}^2\right)^2\right] R_{n1}^2 \\ \quad = \left[\zeta_n^2 + \left(1 - \dfrac{3\Omega_n}{4} R_{n2}^2\right)^2\right] R_{n2}^2 \end{cases} \tag{31}$$

Then we obtain algebraic relations between R_{n1} and R_{n2}:

$$R_{n1}^2 = R_{n2}^2 \tag{32}$$

$$R_{n1}^2 = -\frac{1}{2} R_{n2}^2 + \frac{4}{3\Omega_n} \pm \sqrt{48\Omega_n R_{n2}^2 - 27\Omega_n^2 R_{n2}^2 - 64\zeta_n^2} \tag{33}$$

Equation (33) is not physically relevant as it verifies the third equation of (31) but not the whole system. Then we get

$$R_{n1}^2 = R_{n2}^2 \tag{34}$$

By introducing this result in the system of (27), with $E_n = \Omega_n R_{n1}^2 = \Omega_n R_{n2}^2$ and $E_0 = \Omega_n R_0^2$, after several mathematical manipulations we get

$$\begin{cases} \phi_n^2 E_0 = \left[\zeta_n^2 + \left(1 - \dfrac{3}{4} E_n\right)^2\right] E_n \\ \dfrac{1}{\omega_0^*} \dfrac{dE_n}{dT_1} = -\dfrac{16}{K}\left[\zeta_n^2 + \left(1 - \dfrac{3}{4} E_n\right)^2\right] E_n \zeta^* \\ \quad + \dfrac{-16\zeta_n \phi_n^2 (\alpha_{n,1} + \alpha_{n,2})}{K} E_n \\ K = 16\left(1 + \zeta_n^2\right) - 48 E_n + 27 E_n^2 \end{cases} \tag{35}$$

By rescaling the time and neglecting the damping of the linear system ζ^* in (35) we get

$$\frac{1}{\varepsilon\omega_0^*} \frac{dE_n}{dt} = \frac{-16\zeta_n \phi_n^2 (\alpha_{n,1} + \alpha_{n,2})}{K} E_n \tag{36}$$

which yields to the following function:

$$\begin{aligned} f(E_n) &= \frac{27}{32} E_n^2 - 3E_n + \left(1 + \zeta_n^2\right) \ln(E_n) \\ &= C - \phi_n^2 \zeta_n (\alpha_{n,1} + \alpha_{n,2}) \omega_0^* \varepsilon t \end{aligned} \tag{37}$$

As we saw previously in Sect. 3.1, the denominator K of (36) has real roots if and only if $\zeta_n \leq \frac{1}{\sqrt{3}}$, which is the condition for occurrence of the TET.

3.3 Numerical simulations

In this part, some numerical simulations have been performed in order to compare different analytical predictions of the previous sections with the numerical integration of Eq. (1). These numerical simulations are performed in the case of two parallel NES, attached to the same degree of freedom. We choose the following parameters.

– Initial conditions due to the impulse load:

$$\begin{cases} \dot{q}(0) = 0.1 \text{ m s}^{-1}, \qquad q(0) = 0 \text{ m} \\ x_{n,1}(0) = x_{n,2}(0) = 0 \text{ m} \\ \dot{x}_{n,1}(0) = \dot{x}_{n,2}(0) = 0 \text{ m s}^{-1} \end{cases} \tag{38}$$

– Modal parameters of the master structure:

$$\begin{cases} M_1^* = 1 \text{ kg}, \qquad C_1^* = M_1^* \omega_0^* \zeta^* \text{ N s m}^{-1} \\ K_1^* = (2\pi)^2 \text{ N m}^{-1} \\ \varepsilon\zeta^* = 0.41\%, \qquad \phi_n = 1 \end{cases} \tag{39}$$

– NES parameters:

$$\begin{cases} \mu_{n,1} = \mu_{n,2} = \dfrac{1}{100} M_1^* \text{ kg}, \\ c_{n,1} = c_{n,2} = 0.005 \text{ N s m}^{-1} \\ k_n = k_{n,1} = k_{n,2} = [250; 312; 600] \text{ N m}^{-3} \end{cases} \tag{40}$$

By using this numerical parameters, (29) gives

$$k_n^{\text{opt}} = k_{n,1}^{\text{opt}} = k_{n,2}^{\text{opt}} \approx 312 \text{ N m}^{-3} \tag{41}$$

Numerical simulations and analytical predictions are presented for three different values of k_n, under, above, and near the optimal tuning. Through these simulations, we investigate different mechanisms of control around the optimal design, with unchanged impulse load. Figures 2a, 2c, 2e represent the decreasing of dimensionless variable E_n. These figures show good agreements between analytical prediction of (36) and numerical integration of (2). Figures 2b, 2d, 2f represent the generalized displacement of the main system $q(t)$ with and without the NES device. These figures underline the efficiency of the nonlinear absorber that is able to significantly reduce vibrations of the main system and clearly illustrate the evolution of the absorption efficiency around the optimal tuning value k_n. The analytical prediction of Figs. 2a, 2c, 2e underline the occurrence of multiple solutions near and above the optimal tuning that lead to a sudden jump with high energy dissipation in the main system (see Figs. 2d, 2f). These results show up that these multiple solutions are responsible for the efficiency of the NES. As a conclusion, these NES mechanisms denote that with a nonlinearity under the optimal value we have no multiple solutions and slow dissipation of the main system energy. Near the optimal value, the system quickly goes through the bifurcation that leads to sudden dissipation. Above the optimal value, the system first slowly dissipates energy; this low dissipation phase increases with the nonlinearity of the absorber, before passing through the bifurcation and suddenly decreases. We can conclude that the analytical prediction allows an efficient design of the nonlinear absorber.

4 Under harmonic forcing

In this section, the study of Sect. 3 is extended to the forced system. We investigate the periodic solution of the system in the vicinity of 1:1 resonance. Approximation of the system response, stability and bifurcations are analytically investigated and a tuning criterion is obtained. Then an application with two NES in parallel is analytically and numerically performed for experimental considerations.

Let us consider system of (1), where the linear system is under an harmonic excitation:

$$\begin{cases} M_1^* \ddot{q}_1 + C_1^* \dot{q}_1 + K_1^* q_1 \\ \quad + \displaystyle\sum_{l=1}^{p} \sum_{j=1}^{n_l} \phi_{l,1} \mu_{l,j} \ddot{x}_{l,j} = \sum_{l=1}^{p} \phi_{l,1} F_l(t) \\ \quad \forall n = 1..p, \ \forall j = 1..n_n \\ \mu_{n,j} \ddot{x}_{n,j} + c_{n,j} (\dot{x}_{n,j} - \phi_{n,1} \dot{q}_1) \\ \quad + k_{n,j} (x_{n,j} - \phi_{n,1} q_1)^3 = 0 \end{cases} \tag{42}$$

We consider the system under harmonic forcing then we assume that:

$$\sum_{l=1}^{p} \phi_{l,1} \frac{F_l(t)}{M_1^*} = \varepsilon \omega_0^* F \cos(\omega t) \tag{43}$$

Analysis of harmonic solutions of the system is performed using complexification methods in the vicinity of 1:1 resonance with the external forcing $\varepsilon \omega_0^* F \cos(\omega t)$.

First, we are interested in the design of multiple NES in the forced regime. We introduce global and internal displacements as it follows:

$$\begin{cases} u(t) = q_1(t) \\ v_{n,j} = x_{n,j} - \phi_{n,1} q_1 \quad \forall n = 1..p, \ \forall j = 1..n_n. \end{cases} \tag{44}$$

Equations (42) are written as

$$\begin{cases} \left(\ddot{u} + \omega_0^{*2} u\right) + \varepsilon \lambda^* \dot{u} + \varepsilon \displaystyle\sum_{l=1}^{p} \sum_{j=1}^{n_l} \alpha_{l,j} \phi_{l,j} \ddot{v}_{l,j} \\ \quad + \varepsilon \displaystyle\sum_{l=1}^{p} \sum_{j=1}^{n_l} \alpha_{l,j} \phi_{l,j}^2 \ddot{u}_{l,j} = \varepsilon \omega_0^* F \cos \omega t \\ \left(\ddot{v}_{n,j} + \omega_0^{*2} v_{n,j}\right) + \phi_{n,j} \left(\ddot{u} + \omega_0^{*2} u\right) + \lambda_{n,j} \dot{v}_{n,j} \\ \quad + \Omega_{n,j} \omega_0^{*4} v_{n,j}^3 - \omega_0^{*2} v_{n,j} - \phi_{n,j} \omega_0^{*2} u = 0 \\ \quad \forall n = 1..p, \forall j = 1..n_n \end{cases} \tag{45}$$

Manevitch's complex variables [22] are introduced to investigate periodic solutions in the vicinity of forcing

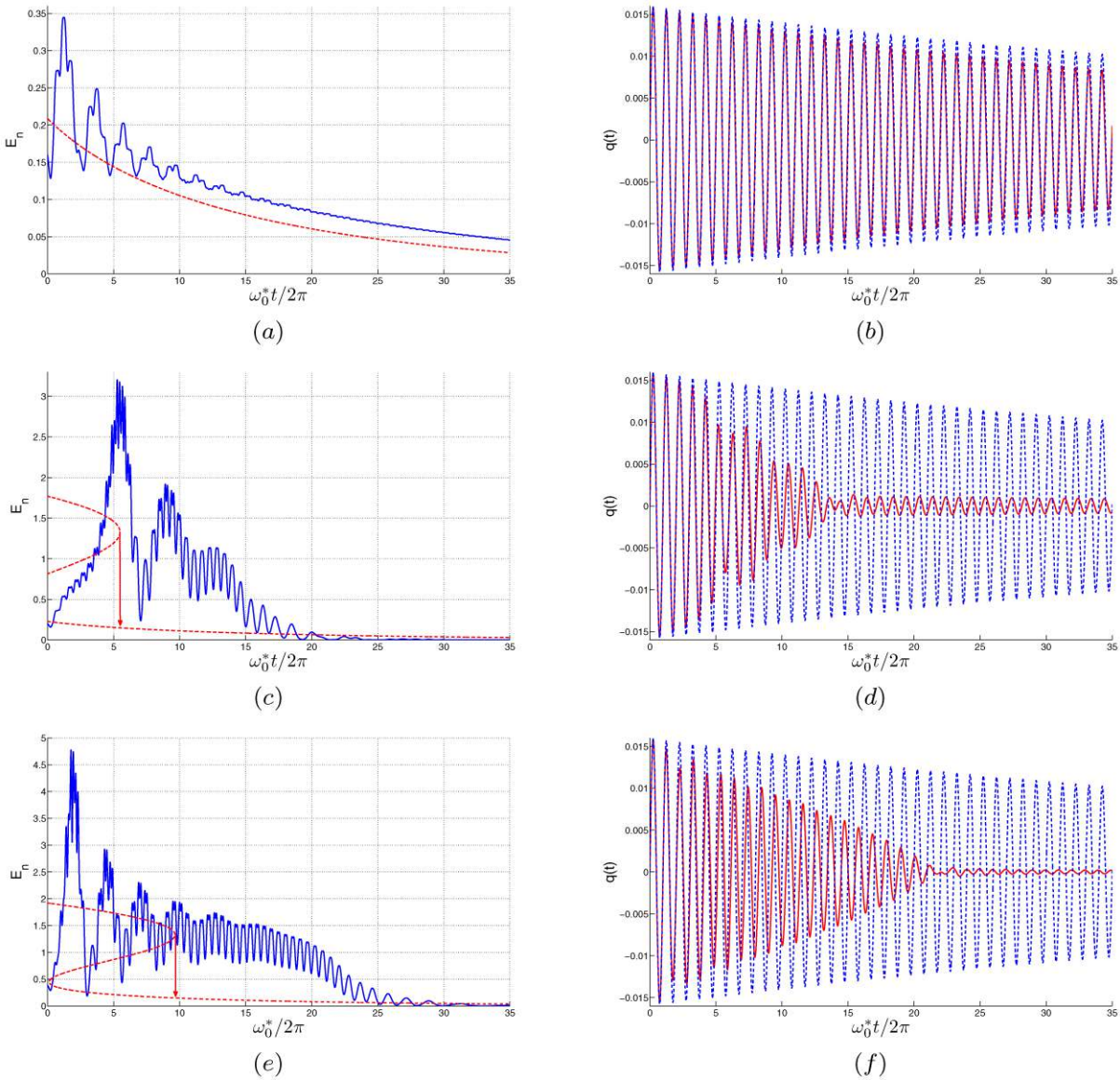

Fig. 2 (**a**, **c**, **e**) Comparison of the absorber efficiency through dimensionless variable E_n for different values of k_n, analytical prediction in dotted line and numerical simulations in *solid line*. (**b**, **d**, **f**) Comparison of master system displacements, coupled with NES in *solid line* and without NES in *dotted line*. (**a**, **b**) $k_n = 250\ \mathrm{N\,m^{-3}}$; (**c**, **d**) $k_n = k^{\mathrm{opt}}$; (**e**, **f**) $k_n = 600\ \mathrm{N\,m^{-3}}$

pulsation ω:

$$\begin{aligned} &\varphi_0 e^{i\omega t} = \dot{u} + i\omega_0^* u \\ &\varphi_{nj} e^{i\omega t} = \dot{v}_{n,j} + i\omega_0^* v_{n,j} \quad \forall n = 1..p,\ \forall j = 1..n_n. \end{aligned} \tag{46}$$

$$\begin{cases} \ddot{u} + \omega_0^{*2} u = \dot{\varphi}_0 e^{i\omega t} + i\left(\omega - \omega_0^*\right)\varphi_0 e^{i\omega t} \\ \quad \forall n = 1..p, \forall j = 1..n_n, \\ \ddot{v}_{n,j} + \omega_0^{*2} v_{n,j} = \dot{\varphi}_{nj} e^{i\omega t} + i(\omega - \omega_0^*)\varphi_{nj} e^{i\omega t} \end{cases} \tag{47}$$

We investigate the response in the vicinity of 1:1 resonance with the external forcing. It is possible to suggest that the evolution of modulation variables φ_0 and φ_{nj} are slow compared to the excitation due to the external force. Under this assumption, first approximation for modulation variables may be obtained by averaging the complexification of (45) with respect to this fast time scale.

We are interested in the design of the NES, so we only consider the $(n_1+n_2+\cdots+n_p)$ last equations of (45). By averaging of these equations one can reach the following system:

$$i\frac{\phi_{n,j}\varepsilon\sigma^*}{2}\varphi_0+i\frac{\varepsilon\sigma^*}{2}\varphi_{nj}+\frac{\zeta_{n,j}}{2}\varphi_{nj}-\frac{3i\Omega_{n,j}}{8}|\varphi_{nj}|^2\varphi_{nj}+\frac{i\phi_{n,j}}{2}\varphi_0+\frac{i}{2}\varphi_{nj}=0\quad\forall n=1..p,\ \forall j=1..n_n \tag{48}$$

with $\frac{\omega}{\omega_0^*}=1+\frac{\varepsilon\sigma^*}{2}$. Steady-state regime of (48) is obtained by demanding:

$$\begin{aligned}&\dot{\varphi}_0=0\\&\dot{\varphi}_{nj}=0,\quad\forall n=1..p,\ \forall j=1..n_n\end{aligned} \tag{49}$$

so,

$$\begin{cases}\forall n=1..p,\ \forall j=1..n_n,\\ (1+\varepsilon\sigma^*)\phi_{n,j}\varphi_0=\left(i\zeta_{n,j}-\left((1+\varepsilon\sigma^*)-\frac{3i\Omega_{n,j}}{4}|\varphi_{nj}|^2\right)\right)\varphi_{nj}\end{cases} \tag{50}$$

By considering the complex conjugate of (50), we obtain:

$$\begin{cases}\forall n=1..p,\ \forall j=1..n_n,\\ \left[\zeta_{n,j}^2+\left(X-\frac{3\Omega_{n,j}}{4}|\varphi_{nj}|^2\right)^2\right]|\varphi_{nj}|^2=\phi_{n,j}^2X^2|\varphi_0|^2\end{cases} \tag{51}$$

where $X=1+\varepsilon\sigma^*$.

By introducing dimensionless variable $Z_{nj}=\Omega_{n,j}|\varphi_{nj}|^2$, we obtain

$$\left[\zeta_{n,j}^2+\left(X-\frac{3}{4}Z_{nj}\right)^2\right]Z_{nj}=\phi_{n,j}^2X^2\Omega_{n,j}|\varphi_0|^2\quad\forall n=1..p,\ \forall j=1..n_n \tag{52}$$

We denote that the principle of separated activity is also verified, in the forced case which permits using the same design method as described in Sect. 3.1. It provides

$$\frac{d\Omega_{n,j}|\varphi_{nj}|^2}{dZ_{n,j}}=\frac{1}{X^2\phi_{n,j}^2}\left[\frac{27}{16}Z_{n,j}^2-3Z_{n,j}+(X^2+\zeta_{n,j}^2)\right] \tag{53}$$

$$\begin{cases}\Delta_F(\zeta)=9X^2-\frac{27}{4}(X^2+\zeta^2)\\ \gamma_F^-(\zeta)=\frac{24X-8\sqrt{\Delta_F(\zeta)}}{27}\end{cases} \tag{54}$$

Then the tuning stiffness for each NES reads as

$$\begin{cases}\forall n=1..p,\ \forall j=1..n_n,\\ k_{n,j}^{\text{opt}}=\frac{\mu_{n,j}\omega_0^{*4}}{\phi_{n,j}^2(1+\varepsilon\sigma^*)^2|\varphi_0|^2}\left(\left[(1+\varepsilon\sigma^*)-\frac{3}{4}\gamma_F^-(\zeta_{n,j})\right]^2+\zeta_{n,j}^2\right)\gamma_F^-(\zeta_{n,j})\end{cases} \tag{55}$$

In the forced case, the main point aims at finding a reasonable value for $|\varphi_0|^2$. Contrary to the impulse load case where initial conditions are known, the steady-state response of the system is unknown. The steady state amplitude of the master system $|\varphi_0|$, seems to depend on variables φ_{nj} and can be obtained by solving (48) and (50), which is not interesting for the design. But if we consider the behavior of a system with the TET, and in particular the energy exchange, it seems that the main system behaves linearly until its energy reaches the energy pumping threshold, and starts to be controlled. We can assume that the steady-state can be obtained by considering that the system behaves linearly until the energy pumping threshold is reached.

Under this assumption, we will tune the NES under harmonic forcing by considering:

$$\begin{aligned}|\varphi_0|^2&\approx(\dot{u}^2+\omega_0^{*2}u^2)_{\text{statio}}\\&\approx\omega_0^{*2}u_{\text{statio}}^2\\&\approx\frac{\varepsilon^2\omega_0^{*2}F^2}{(\omega_0^*-\tilde{\omega})^2+\tilde{\omega}^2\varepsilon\lambda^*}\end{aligned} \tag{56}$$

where $\tilde{\omega}$ is the cut pulsation, i.e., the pulsation which triggers the TET and u_{statio} (the stationary value for displacement $u(t)$) at pulsation $\tilde{\omega}$.

4.1 Case of two NES in parallel under harmonic forcing

In this part, we consider the simple case of two parallel NES that are attached at dof with the mode shapes $\phi_{n,1}$ and $\phi_{n,2}$. Mass, damping, and stiffness of each NES are $(\mu_{n,1},\mu_{n,2})$, $(c_{n,1},c_{n,2})$, and $(k_{n,1},k_{n,2})$, respectively.

In this case, (45) can be rewritten as

$$\begin{cases} \left(\ddot{u}+\omega_0^{*2}u\right)+\varepsilon\lambda^*\dot{u}+\varepsilon\alpha_{n,1}\phi_{n,1}\ddot{v}_{n,1} \\ \quad +\varepsilon\alpha_{n,2}\phi_{n,2}\ddot{v}_{n,2}+\varepsilon Y_2\ddot{u}=\varepsilon\omega_0^* F\cos\omega t, \\ \left(\ddot{v}_{n,1}+\omega_0^{*2}v_{n,1}\right)+\phi_{n,1}\left(\ddot{u}+\omega_0^{*2}u\right)+\lambda_{n,1}\dot{v}_{n,1} \\ \quad +\Omega_{n,1}\omega_0^{*4}v_{n,1}^3-\omega_0^{*2}v_{n,1}-\phi_{n,1}\omega_0^{*2}u=0, \\ \left(\ddot{v}_{n,2}+\omega_0^{*2}v_{n,2}\right)+\phi_{n,2}\left(\ddot{u}+\omega_0^{*2}u\right)+\lambda_{n,2}\dot{v}_{n,2} \\ \quad +\Omega_{n,2}\omega_0^{*4}v_{n,2}^3-\omega_0^{*2}v_{n,2}-\phi_{n,2}\omega_0^{*2}u=0 \end{cases} \tag{57}$$

with $Y_2=\alpha_{n,1}\phi_{n,1}^2+\alpha_{n,2}\phi_{n,2}^2$.
By introducing complex variables and averaging equations in the vicinity of 1:1 resonance with the external forcing we obtain the following system of equations:

$$\begin{cases} (1+\varepsilon Y_2)\left(\frac{1}{\omega_0^*}\dot{\varphi}_0+i\left(\frac{\omega}{\omega_0^*}-1\right)\varphi_0\right)+\varepsilon\alpha_{n,1}\phi_{n,1} \\ \quad \times\left(\frac{1}{\omega_0^*}\dot{\varphi}_{n1}+i\left(\frac{\omega}{\omega_0^*}-1\right)\varphi_{n1}\right)+\alpha_{n,2}\phi_{n2}\varepsilon \\ \quad \times\left(\frac{1}{\omega_0^{*2}}\dot{\varphi}_{n2}+i\left(\frac{\omega}{\omega_0^*}-1\right)\varphi_{n2}\right)+\frac{\varepsilon\zeta^*}{2}\varphi_0 \\ \quad +\frac{i\varepsilon\phi_{n,1}}{2}\varphi_{n1}+\frac{i\alpha_{n,2}\varepsilon\phi_{n,2}}{2}\varphi_{n2}+\frac{i\varepsilon}{2}Y_2\varphi_0=\frac{\varepsilon F}{2} \\ \phi_{n,1}\left(\frac{1}{\omega_0^*}\dot{\varphi}_0+i\left(\frac{\omega}{\omega_0^*}-1\right)\varphi_0\right) \\ \quad +\left(\frac{1}{\omega_0^*}\dot{\varphi}_{n1}+i\left(\frac{\omega}{\omega_0^*}-1\right)\varphi_{n1}\right)+\frac{\zeta_{n,1}}{2}\varphi_{n1} \\ \quad -\frac{3i\Omega_{n,1}}{8}|\varphi_{n1}|^2\varphi_{n1}+\frac{i\phi_{n,1}}{2}\varphi_0+\frac{i}{2}\varphi_{n1}=0 \\ \phi_{n,1}\left(\frac{1}{\omega_0^*}\dot{\varphi}_0+i\left(\frac{\omega}{\omega_0^*}-1\right)\varphi_0\right) \\ \quad +\left(\frac{1}{\omega_0^*}\dot{\varphi}_{n,2}+i\left(\frac{\omega}{\omega_0^*}-1\right)\varphi_{n2}\right)+\frac{\zeta_{n,2}}{2}\varphi_2 \\ \quad -\frac{3i\Omega_{n,2}}{8}|\varphi_{n2}|^2\varphi_{n2}+\frac{i\phi_{n,2}}{2}\varphi_0+\frac{i}{2}\varphi_{n2}=0 \end{cases} \tag{58}$$

We investigate the stationary response regime by requiring:

$$\dot{\varphi}_0=\dot{\varphi}_{n1}=\dot{\varphi}_{n2}=0 \tag{59}$$

which yield to the following system:

$$\begin{cases} (1+\varepsilon Y_2)i\sigma^*\varphi_0+\varepsilon\alpha_{n,1}\phi_{n,1}i\sigma^*\varphi_{n1} \\ \quad +\alpha_{n,2}\phi_{n,2}\varepsilon i\sigma^*\varphi_{n2}+\zeta^*\varphi_0+i\alpha_{n,1}\phi_{n,1}\varphi_{n1} \\ \quad +i\alpha_{n,2}\phi_{n,2}\varphi_{n2}+iY_2\varphi_0=F \\ i\frac{\phi_{n,1}\varepsilon\sigma^*}{2}\varphi_0+i\frac{\varepsilon\sigma^*}{2}\varphi_{n1}+\frac{\zeta_{n,1}}{2}\varphi_{n1} \\ \quad -\frac{3i\Omega_{n,1}}{8}|\varphi_{n1}|^2\varphi_{n1}+\frac{i\phi_{n,1}}{2}\varphi_0+\frac{i}{2}\varphi_{n1}=0 \\ i\frac{\phi_{n,2}\varepsilon\sigma^*}{2}\varphi_0+i\frac{\varepsilon\sigma^*}{2}\varphi_{n2}+\frac{\zeta_{n,2}}{2}\varphi_{n2} \\ \quad -\frac{3i\Omega_{n,2}}{8}|\varphi_{n2}|^2\varphi_{n2}+\frac{i\phi_{n,2}}{2}\varphi_0+\frac{i}{2}\varphi_{n2}=0 \end{cases} \tag{60}$$

By introducing $Z_{n10}=\Omega_{n,1}|\varphi_0|^2$, $Z_{n20}=\Omega_{n,2}|\varphi_0|^2$, $Z_{n22}=\Omega_{n,2}|\varphi_{n22}|^2$, $Z_{n11}=\Omega_{n,1}|\varphi_{n1}|^2$ and using polar form and calculating modulus, one can find the following dimensionless equations:

$$\begin{cases} \left[\left[(1+\varepsilon\sigma^*)-\frac{3}{4}Z_{n11}\right]^2+\zeta_{n,1}^2\right]Z_{n11} \\ \quad =\phi_{n,1}^2(1+\varepsilon\sigma^*)^2Z_{n10} \\ \left[\left[(1+\varepsilon\sigma^*)-\frac{3}{4}Z_{n22}\right]^2+\zeta_{n,2}^2\right]Z_{n22} \\ \quad =\phi_{n,2}^2(1+\varepsilon\sigma^*)^2Z_{n20} \end{cases} \tag{61}$$

Let us consider the case of two parallel NES which are attached at the same dof, with the same damping ($\phi_{n,1}=\phi_{n,2}=\phi_n$ and $\zeta_{n,1}=\zeta_{n,2}=\zeta_n$). The NES are attached to the same dof in order to make a comparison with experimental results which are given in the companion paper; nevertheless, the following analytical study could be undertaken for $\phi_{n,1}\neq\phi_{n,2}$ with similar method. As in the previous section, the two NES are tuned on the same level of activation:

$$\frac{k_{n,1}}{\mu_{n,1}}=\frac{k_{n,2}}{\mu_{n,2}} \quad\Rightarrow\quad \Omega_{n,1}=\Omega_{n,2}=\Omega_n \tag{62}$$

Then we obtain algebraic relations between Z_{n11} and Z_{n22}:

$$Z_{n11}=Z_{n22} \tag{63}$$

$$Z_{n11}=-\frac{1}{2}Z_{n22}+\frac{4X}{3} \pm\frac{1}{6}\sqrt{48XZ_{n22}-27Z_{n22}^2-64\zeta_n^2} \tag{64}$$

Equation (64) is not physically relevant as it verifies the third equation of (61) but does not verify the whole system. Then we have:

$$|\varphi_{n1}|^2 = |\varphi_{n2}|^2 \quad \Rightarrow \quad \varphi_{n1} = \varphi_{n2} \quad \text{(see (60))} \tag{65}$$

and the following reduced system:

$$\begin{cases} (i[XY+\sigma^*]+\zeta^*)\varphi_0 + \dfrac{i}{\phi_n} XY\varphi_{n1} = F \\ iX\phi_n\varphi_0 + iX\varphi_{n1} - \dfrac{3i\Omega_n}{4}|\varphi_{n1}|^2\varphi_{n1} + \zeta_n\varphi_{n1} = 0 \end{cases} \tag{66}$$

After some mathematical manipulations the behavior of the system in terms of φ_{n1} can be expressed as:

$$\begin{cases} \dfrac{i\phi_n X F(\zeta_n - i[XY+\sigma^*])}{K} \\ \quad = \left[i\left(\dfrac{X^2Y[XY+\sigma^*]}{K} - X + \dfrac{3\Omega_n}{4}|\varphi_{n1}|^2 \right) \right. \\ \quad \left. - \left(\dfrac{X^2Y}{K}\zeta^* + \zeta_n \right) \right] \varphi_{n1} \\ K = (XY+\sigma^*)^2 + \zeta^{*2} \end{cases} \tag{67}$$

By evaluating the modulus, we find:

$$\frac{\phi_n^2 X^2 Z_F}{K} = \left[\left(\frac{X^2Y[XY+\sigma^*]}{K} - X + \frac{3}{4}Z_n \right)^2 + \left(\frac{X^2Y}{K}\zeta^* + \zeta_n \right)^2 \right] Z_n$$

$$\text{with } Z_F = \Omega_n|\varphi_0|^2 \text{ and } Z_n = \Omega_n|\varphi_{n1}|^2. \tag{68}$$

Equation (68) is polynomial of order 3 in terms of Z_n. It can be written under the following general form:

$$\begin{cases} p_3 Z_n^3 + p_2 Z_n^2 + p_1 Z_n + p_0 = 0 \quad \text{with:} \\ p_3 = \dfrac{9}{16} \\ p_2 = -\dfrac{3X}{2} + (\sigma^* + XY)\dfrac{3X^2Y}{2K} \\ p_1 = (X^2 + \zeta^{*2}) + \dfrac{2X^2Y}{K}(\zeta_n\zeta^* - \sigma^* + X - X^2Y) \\ \qquad + \dfrac{X^4Y^2}{K^2}(\zeta^{*2} + (\sigma^* + XY)^2) \\ p_0 = -\dfrac{\phi_n^2 X^2 Z_F}{K} \end{cases} \tag{69}$$

Roots of this polynomial are the values of Z_n at each step of frequency. The behavior of the main system can be expressed by the following system:

$$Z_F = \frac{1}{\phi_n^2(1+\varepsilon\sigma^*)^2}\left[\left[(1+\varepsilon\sigma^*) - \frac{3}{4}Z_n \right]^2 + \zeta_n^2 \right] Z_n, \tag{70}$$

$$u^2_{\text{statio}} \approx \frac{Z_F}{\omega_0^* \Omega_n}.$$

4.2 Multiple solutions and linear stability analysis

4.2.1 Multiplicity of periodic solutions

The polynomial of (69) can exhibit multiple solutions. We will investigate the case of the shift between one single real solution to three real solutions. The polynomial of (69) reads as

$$p_3 Z_n^3 + p_2 Z_n^2 + p_1 Z_n + p_0 = 0 \tag{71}$$

which can be written in the Cardan form:

$$\begin{cases} T^3 + pT + q = 0 \quad \text{with} \\ p = \dfrac{p_1}{p_3} - \dfrac{p_2^2}{3p_3^2} \\ q = \dfrac{p_2}{27p_3}\left(\dfrac{2p_2^2}{p_3} - \dfrac{9p_1}{p_3} \right) + \dfrac{p_0}{p_3} \end{cases} \tag{72}$$

According to the Cardan formulas the double roots $\bar{T}$ can be expressed as

$$\bar{T} = \frac{-3q}{2p} \quad \Rightarrow \quad \bar{Z}_n = \frac{p_1p_2 - 9p_3p_0}{6p_1p_3 - 2p_2^2} \tag{73}$$

As a double root $\bar{Z}_n$ is also solution of the first derivative of (71):

$$3p_3\bar{Z}_n + 2p_2\bar{Z}_n + p_1 = 0 \tag{74}$$

Combination of (73) and (74) gives the following equation for the border between single periodic solution and three periodic solutions:

$$\begin{aligned} &3p_3(p_1p_2 - 9p_3p_0)^2 \\ &\quad + 2p_2(p_1p_2 - 9p_3p_0)\left(6p_1p_3 - 2p_2^2\right) \\ &\quad + p_1\left(6p_1p_3 - 2p_2^2\right)^2 = 0 \end{aligned} \tag{75}$$

4.2.2 Linear stability analysis

To prevent the system from unpredicted behaviors, the stability of fixed points of (58), i.e., solutions of polynomial of (69) must be investigated. By introducing (65) in (58) can be rewritten as

$$\begin{cases} (1+\varepsilon Y_2)\left(\frac{1}{\omega_0^*}\dot{\varphi}_0+\frac{i\varepsilon\sigma^*}{2}\varphi_0\right)+\frac{\varepsilon Y}{\phi_n}\left(\frac{1}{\omega_0^*}\dot{\varphi}_{n1}\right. \\ \quad \left.+\frac{i\varepsilon\sigma^*}{2}\varphi_{n1}\right)+\varepsilon\left(\frac{\zeta^*}{2}+iY\right)\varphi_0+\frac{i\varepsilon Y_2}{2\phi_n}\varphi_{n1}=0 \\ \phi_n\left(\frac{1}{\omega_0^*}\dot{\varphi}_0+\frac{i\varepsilon\sigma^*}{2}\varphi_0\right)+\left(\frac{1}{\omega_0^*}\dot{\varphi}_{n1}+\frac{i\varepsilon\sigma^*}{2}\varphi_{n1}\right) \\ \quad +\frac{\zeta_n}{2}\varphi_{n1}-\frac{3i\Omega_n}{8}|\varphi_{n1}|^2\varphi_{n1}+\frac{i\phi_n}{2}\varphi_0+\frac{i}{2}\varphi_{n1}=0 \end{cases} \tag{76}$$

We first linearize (58) in the vicinity of the steady-state response to investigate the stability of fixed points. Let us introduce small perturbations to the fixed points as it follows:

$$\begin{cases} \varphi_0=\varphi_{00}+\chi_0 \quad |\chi_0|\ll|\varphi_{00}| \\ \varphi_{n1}=\varphi_{n10}+\chi_{n1} \quad |\chi_{n1}|\ll|\varphi_{n10}| \end{cases} \tag{77}$$

By progressing until second-order expansions, the system of linearized equations can be expressed as

$$\begin{cases} (1+\varepsilon Y_2)\left(\frac{1}{\omega_0^*}\dot{\chi}_0+\frac{i\varepsilon\sigma^*}{2}\chi_0\right)+\frac{\varepsilon Y_2}{\phi_n}\left(\frac{1}{\omega_0^*}\dot{\chi}_{n1}\right. \\ \quad \left.+\frac{i\varepsilon\sigma^*}{2}\chi_{n1}\right)+\varepsilon\left(\frac{\zeta^*}{2}+iY\right)\chi_0+\frac{i\varepsilon Y_2}{2\phi_n}\chi_{n1}=0, \\ \phi_n\left(\frac{1}{\omega_0^*}\dot{\chi}_0+\frac{i\varepsilon\sigma^*}{2}\chi_0\right)+\left(\frac{1}{\omega_0^*}\dot{\chi}_{n1}+\frac{i\varepsilon\sigma^*}{2}\chi_{n1}\right) \\ \quad +\frac{\zeta_n}{2}\chi_{n1}-\frac{3i\Omega_n}{8}\varphi_{n10}^2\bar{\chi}_{n1}-\frac{3i\Omega_n}{4}|\varphi_{n10}|^2\chi_{n1} \\ \quad +\frac{i\phi_n}{2}\chi_0+\frac{i}{2}\chi_{n1}=0 \end{cases} \tag{78}$$

Equation (78) is a linear system which can be written in a matrix form as

$$\begin{pmatrix} \dot{\chi}_0 \\ \dot{\chi}_{n1} \\ \dot{\bar{\chi}}_0 \\ \dot{\bar{\chi}}_{n1} \end{pmatrix}=A\begin{pmatrix} \chi_0 \\ \chi_{n1} \\ \bar{\chi}_0 \\ \bar{\chi}_{n1} \end{pmatrix} \tag{79}$$

where

$$A=\omega_0^*\begin{pmatrix} a_{11} & a_{12} & 0 & a_{14} \\ a_{21} & a_{22} & 0 & a_{24} \\ 0 & \bar{a}_{14} & \bar{a}_{11} & \bar{a}_{12} \\ 0 & \bar{a}_{24} & \bar{a}_{21} & \bar{a}_{22} \end{pmatrix} \tag{80}$$

and

$$\begin{aligned} a_{11}&=-\frac{\varepsilon}{2}\big(i(\sigma+Y)+\zeta_0\big) \\ a_{12}&=\left[\frac{\varepsilon Y(2\zeta_a-3i\Omega_a|\varphi_{n10}|^2)}{4\phi_a}\right] \\ a_{14}&=-\frac{3i\Omega_a\varepsilon Y}{\phi_a}\varphi_{10} \\ a_{21}&=\left[-\frac{i}{2}\phi_a(1+\varepsilon Y)+\frac{\varepsilon\phi_a}{2}\zeta_0+i\varepsilon\phi_a Y\right] \\ a_{22}&=\left[\left(-\frac{X}{2}+\frac{3i\Omega_a}{4}|\varphi_{n10}|^2-\frac{\zeta_a}{2}\right)\right. \\ &\quad \left.\times(1+\varepsilon Y)+\frac{\varepsilon XY}{2}\right] \\ a_{24}&=\left[\frac{3i\Omega_a}{8}(1+\varepsilon Y)\varphi_{n10}\right] \end{aligned} \tag{81}$$

Then we can evaluate the characteristic equation of the matrix A which is a 4th order polynomial in terms of θ with coefficient depending on variable $Z_n=\Omega_n|\varphi_{n1}|^2$:

$$\begin{aligned} P(\theta)=\theta^4+\big[(1+\varepsilon Y)\zeta_a+\varepsilon\zeta_0\big]\theta^3+g_2\big(Z_n^2,Z_n\big)\theta^2 \\ +g_1\big(Z_n^2,Z_n\big)\theta+g_0\big(Z_n^2,Z_n\big) \end{aligned} \tag{82}$$

where $g_2(Z_n^2,Z_n)$, $g_1(Z_n^2,Z_n)$ and $g_0(Z_n^2,Z_n)$ are functions which depend on variables Z_n^2 and Z_n. By investigating the real parts of roots of polynomial function $P(\theta)$ of (82), we can establish the stability of the different solutions. A Routh–Hurwitz criterion is used to establish stable and unstable areas. To investigate the equation of the Hopf bifurcation, we look for purely imaginary eigenvalues of matrix A. Let us introduce

$$\theta=\pm i\beta \tag{83}$$

Equation (82) gives

$$\beta^4-g_1\beta^2+g_0=0 \tag{84}$$

$$-\big[(1+\varepsilon Y)\zeta_a+\varepsilon\zeta_0\big]\beta^3+g_2\beta=0 \tag{85}$$

According to (85),

$$\beta\left(g_2 - \left[(1+\varepsilon Y)\zeta_a + \varepsilon\zeta_0\right]\beta^2\right) = 0 \tag{86}$$

$\beta = 0$ corresponds to the case $Z_F = 0$, which is the unforced case and was studied previously; then we get

$$\beta = \pm\sqrt{\frac{g_2}{[(1+\varepsilon Y)\zeta_a + \varepsilon\zeta_0]}} \tag{87}$$

By introducing this result in (84), we obtain the border of the Hopf bifurcation:

$$\begin{cases} g_2^2 - g_1 g_2[(1+\varepsilon Y)\zeta_a + \varepsilon\zeta_0] \\ \quad + g_3[(1+\varepsilon Y)\zeta_a + \varepsilon\zeta_0]^2 = 0 \\ p_3 Z_n^3 + p_2 Z_n^2 + p_1 Z_n + p_0 = 0 \end{cases} \tag{88}$$

4.3 Numerical simulations

In this part, numerical simulations are performed in order to compare analytical predictions of Sect. 4.1 with numerical integration of (1). These numerical simulations are performed for the case of two parallel NES which are attached to the same degree-of-freedom. System parameters are given by:

– Initial conditions before harmonic excitation:

$$\begin{cases} \dot{q}(0) = 0\ \mathrm{m\,s^{-1}}, \qquad q(0) = 0\ \mathrm{m} \\ x_{n,1}(0) = x_{n,2}(0) = 0\ \mathrm{m}, \\ \dot{x}_{n,1}(0) = \dot{x}_{n,2}(0) = 0\ \mathrm{m\,s^{-1}} \end{cases} \tag{89}$$

– Amplitude of the external excitation:

$$F = 0.36\ \mathrm{m\,s^{-1}} \tag{90}$$

– Modal parameters of the master structure:

$$\begin{cases} M_1^* = 0.835\ \mathrm{kg}, \\ C_1^* = M_1^*\omega_0^*\zeta^*\ \mathrm{N\,s\,m^{-1}} \\ K_1^* = (2\pi \times 4.26)^2\ \mathrm{N\,m^{-1}}, \\ \varepsilon\zeta^* = 3\%,\ \phi_n = 1 \end{cases} \tag{91}$$

– NES parameters:

$$\begin{cases} \mu_{n,1} = \mu_{n,2} = 0.03\ \mathrm{kg} \\ c_{n,1} = c_{n,2} = 0.25\ \mathrm{N\,s\,m^{-1}} \\ k_{n,1} = k_{n,2} = [0.6;\ 1.8;\ 3.2;\ 3.5] \times 10^5\ \mathrm{N\,m^{-3}}. \end{cases} \tag{92}$$

– Level of activation and tuning calculated from (55):

$$\begin{cases} \textit{Cut frequency}: \\ \quad \dfrac{\tilde{\omega}}{\omega_0^*} = \{0.91,\ 1.08\}\ (\textit{Frf level}: 5.65) \\ \quad \Rightarrow k_n^{\mathrm{opt}} \approx 1.76 \times 10^5\ \mathrm{N\,m^{-3}} \end{cases} \tag{93}$$

where the cut frequency $\tilde{\omega}$ defines the intersection between the chosen activation threshold and the linear Frf of the system.

Modal shape has been normalized with respect to the infinite norm of mode shapes. The modal parameters represent the first mode modal parameters of a four storey prototype structure which is used for experimental test in the companion paper. As we are considering the first mode and the two NES are attached to the last storey of the structure, we have $\phi_n = 1$. For external excitation, we do not consider any initial conditions on the system and we investigate the system under an harmonic excitation with the amplitude of $F = 0.36\ \mathrm{m\,s^{-1}}$, where F is the same amplitude which is considered in (45). Since the system is under harmonic forcing, then we are interested to consider the system in the frequency domain. We study the frequency response of the system in the vicinity of 1:1 resonance for three different nonlinearity values around an optimal value. Contrary to the transient case the optimal value is not unique and is determined through a chosen threshold, represented by the linear behavior level of FrF at the chosen cut pulsation $\tilde{\omega}$. This threshold is investigated in Figs. 3, 4, and 5, with cut pulsation $\frac{\tilde{\omega}}{\omega_0^*} = \{0.91, 1.08\}$. Let us analyze the frequency response of the structure. We suppose that F is invariable and we change the nonlinearity of the NES k_n. Figures 3, 4, and 5 represent the frequency response function in the vicinity of pulsation ω_0^* for values of k_n under (Fig. 3a), above (Figs. 4a, 4b and 5a, 5b) and near the optimal value k^{opt} (Fig. 3b). In these figures, we can observe the theoretical linear behavior of the main structure in dashed line, the analytical prediction of the nonlinear behavior which is obtained from (69) in solid line, and the numerical integration of (42) with circles markers. The numerical integration is computed with a Matlab RK45 scheme, data are taken during the stationary regime, after enough periods of excitation. At each increment of frequency, the initial conditions are the conditions of the previous point in the frequency sweep. This numerical sweep goes from low to high frequencies.

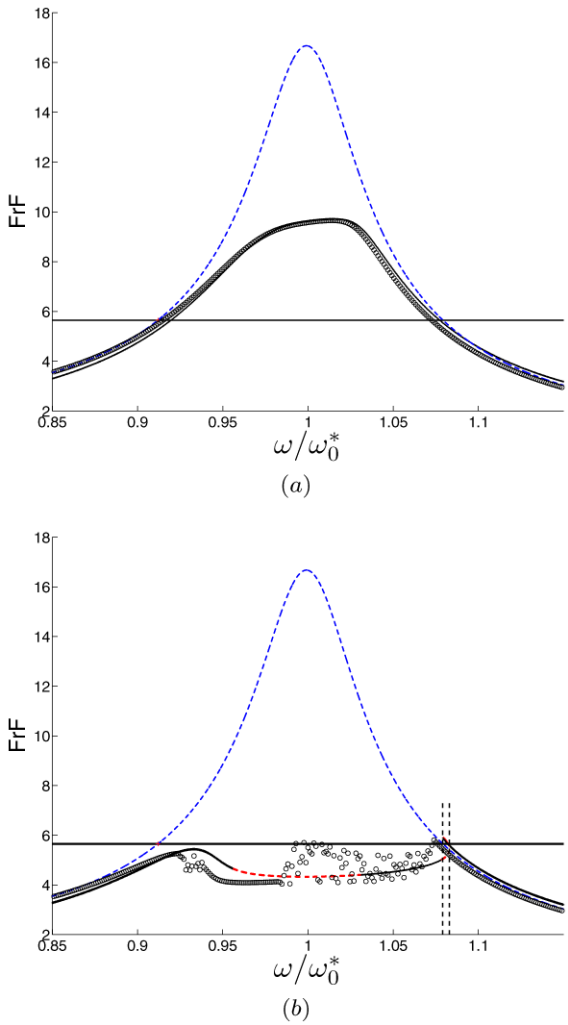

Fig. 3 FrF of the system in the vicinity of 1:1 resonance for different value of k_n. (**a**) $k_n = 6 \times 10^4$ N m^{-3}; (**b**) $k_n = 1.76 \times 10^5$ N m$^{-3} \approx k^{\text{opt}}$. ($-\ -\ -$) analytical linear behavior, (—) analytical prediction (stable), (-.-.-.-) analytical prediction (unstable), ($\circ\ \circ\ \circ$) numerical integration

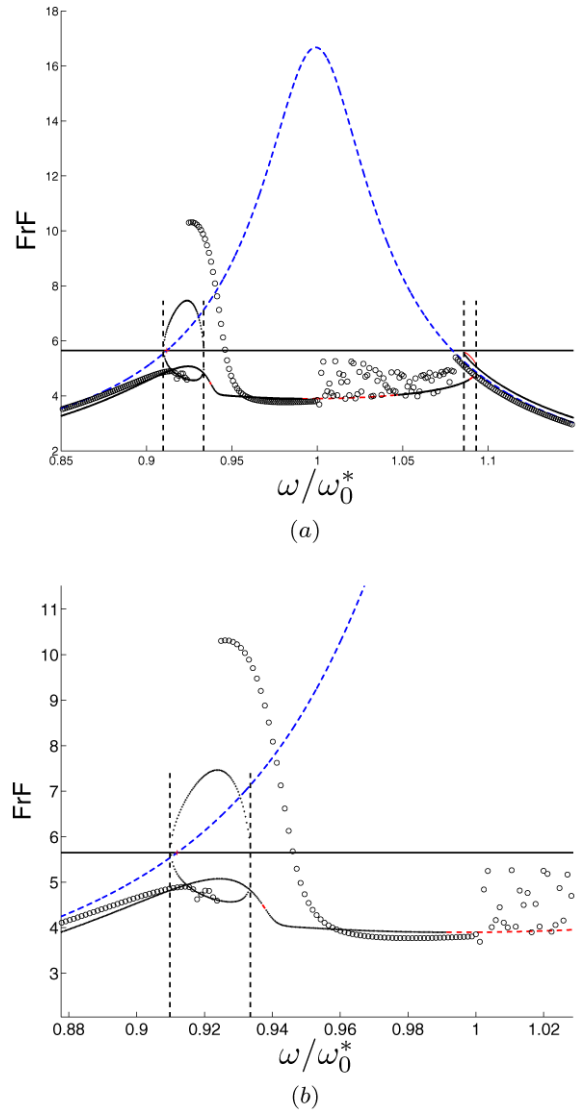

Fig. 4 (**a**) FrF of the system in the vicinity of 1:1 resonance for $k_n = 2 \times 10^5$ N m^{-3}; (**b**) Magnification on the range of pulsation [0.88;1.02] ($-\ -\ -$) analytical linear behavior, (—) analytical prediction (stable), (-.-.-.-) analytical prediction (unstable), ($\circ\ \circ\ \circ$) numerical integration

The stability of multiple analytical solutions is highlighted: stable periodic solutions are in solid line and unstable are plotted with dash-dot line. Multiple solutions areas are identified by vertical dotted lines and the chosen activation threshold is plotted with an horizontal solid line.

The influence of variable k_n on the behavior of the system is demonstrated in Figs. 3, 4, and 5. By increasing the stiffness of the nonlinear absorber, the frequency response decreases and the resonance peak breaks until the optimal design. This optimal design defined through a displacement threshold that is illustrated in Figs. 3, 4, and 5 with an horizontal solid line. It is obvious that the structure behaves linearly until it reaches the cut frequency, then strong nonlinear behavior occurs; the resonance peak is broken and the system is kept under the desired threshold, until it passes the resonance and behaves linearly again. Figure 3b illustrates the case of the optimal choice, when the NES is tuned on the chosen threshold. Figure 4a,

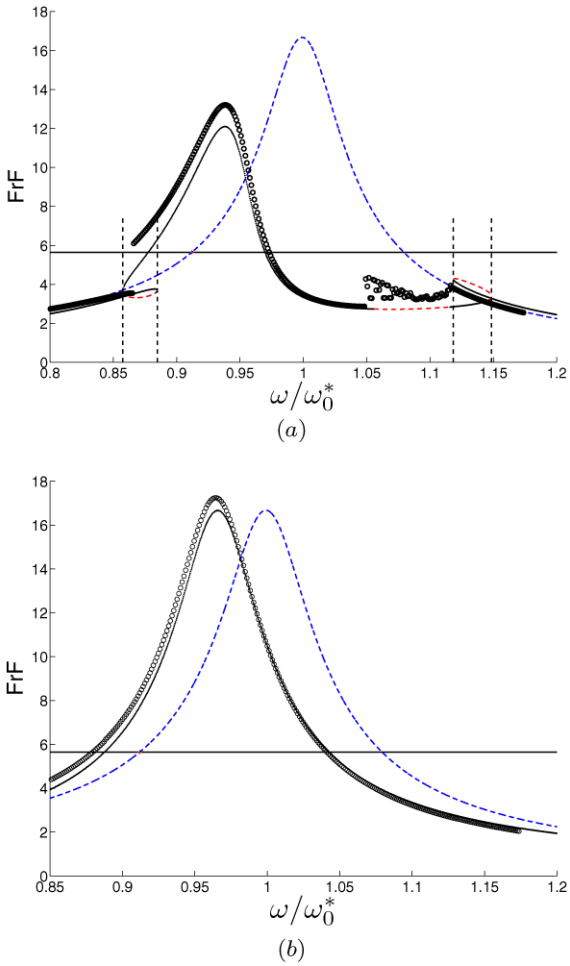

Fig. 5 FrF of the system in the vicinity of 1:1 resonance for high value of k_n. (**a**) $k_n = 3.5 \times 10^5$ N m^{-3}; (**b**) $k_n \to +\infty$ ($-\ -\ -$) analytical linear behavior, (—) analytical prediction (stable), (-.-.-.-) analytical prediction (unstable), ($\circ\ \circ\ \circ$) numerical integration

4b illustrate the case of a nonlinearity above the optimal design, or for a low cut frequency.

We denote that the frequency response remains at a low level, but also the occurrence of a bifurcation with a stable closed loop (see Figs. 4a, 4b) which appears for under resonance frequencies. This loop represents a risk, as the system can be possibly attracted on a stable solution with an amplitude that overcomes the desired threshold. By increasing the nonlinear stiffness this loop grows up (see Fig. 5a), until it generates a new resonant peak. If the nonlinear connection is increased until an infinite rigidity between the linear system and the additional absorbers masses this new peak turns out to the initial linear resonance peak shifted

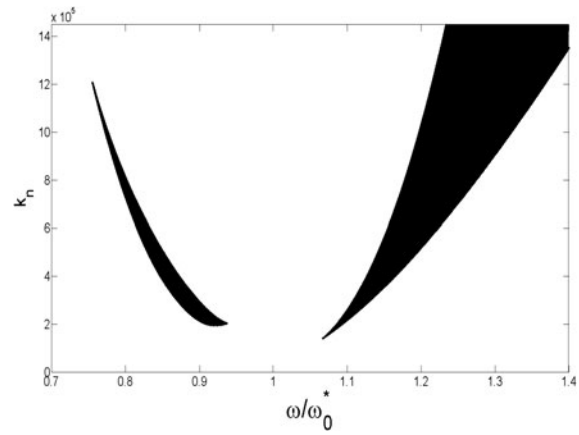

Fig. 6 Evolution of the multiplicity of periodic solutions in the plane (ω/ω_0^*, k_n)

to low frequencies because of the embedded mass to the main system, as presented in Fig. 5b. The occurrence of this new resonant peak reduces the efficiency of the control and can be dangerous for the system, but the occurrence of the phenomenon can be predicted by studying the multiplicity of the periodic solution of the system calculated in (75) and represented in Fig. 6.

We denote also that the analytical prediction represented Figs. 3 and 5 are in good agreement with the numerical simulations; we notice that in the unstable areas numerical results suggest that the system has no periodic solutions.

Nevertheless, in Fig. 4, the analytical prediction is slightly different from numerical simulations. This phenomenon occurs only for a small range of nonlinear stiffness and represents the transition between the close loop and the secondary resonant peak. From the numerical simulations, which give a smooth curve, we can suggest that significant contribution of harmonics and/or secondary resonance stable phenomenons are involved in this area. It means that for this range of frequencies and stiffness 1:1 resonance assumption is not correct, and unable to predict the numerical branch that appears. This specificity could be investigated more deeply. Indeed, we do not study this case here as the phenomenon does not correspond to an interesting value of stiffness for a good tuning of the NES.

Figure 6 represents the evolution of the multiplicity of the periodic solutions in the plane $(k_n, \frac{\omega}{\omega_0^*})$ which is obtained from (75). The shadowed areas represent stiffnesses which inject three periodic solutions to the

system under consideration and the rest part represent the system with single periodic solutions. The detected zones in this figure give us a good idea in choosing the right nonlinear stiffness and predicting the behavior of the system according to the chosen k_n. This diagram predicts, for example, the emergence of the loop presented in Fig. 4. Here, we notice that the first multiplicity of solution appears in the vicinity of $k_n \approx 1.4 \times 10^5\ \mathrm{N\,m^{-3}}$, above the resonance frequency, the second area of multiple solutions appears in the vicinity of $k_n \approx 1.94 \times 10^5\ \mathrm{N\,m^{-3}}$, which is in good agreement with the behavior of the system which is presented in Figs. 3b and 4. This argument indicates the complex and important influence of the NES on the overall behavior of the system during the TET and allow us to prevent from hazardous and uncommon behaviors.

5 Conclusion

An analytical tuning of NES devices is proposed for controlling strong modes of linear master structure by using the TET phenomenon. This method is based on the study of the bifurcation that occurs during the TET and is investigated for systems under transient and harmonic excitations. Necessary conditions for appropriate TET are highlighted and different mechanisms are considered and commented upon. The efficiency of a system of parallel NES compared to a single NES system is also underlined for the transient and forced cases. Even if the effect of NES damping is not so clear in the forced case the main conclusions are that parallel NES offer better repartition of masses, multiple levels of activation, lower the required nonlinear stiffness, and finally results are more efficient. Obtained theoretical results are endowed in the companion paper to control the first mode of a four storey structure with two parallel NES at the last floor.

Acknowledgements This work has been supported by French National Research Agency under the contract ANR-07-BLAN-0193

References

1. Silva, C.D.: Vibration and Shock Handbook. CRC Press, Boca Raton (2005)
2. Vakakis, A.F.: Inducing passive nonlinear energy sink in vibrating systems. J. Vib. Acoust. **123**(3), 324–332 (2001)
3. Gendelman, O., Manevitch, L., Vakakis, A., M'Closkey, R.: Energy pumping in nonlinear mechanical oscillators. Part 1. Dynamics of the underlying Hamiltonian systems. J. Appl. Mech. **68**, 42–48 (2001)
4. Vakakis, A., Gendelman, O.: Energy pumping in nonlinear mechanical oscillators. Part 2. Resonance capture. J. Appl. Mech. **68**, 34–41 (2001)
5. Vakakis, A.: Shock isolation through the use of nonlinear energy sinks. J. Vib. Control **12**, 355–371 (2003)
6. Gendelman, O.: Bifurcations of nonlinear normal modes of linear oscillator with strongly nonlinear damped attachment. Nonlinear Dyn. **37**(2), 115–128 (2004)
7. Gendelman, O., Lamarque, C.-H.: Dynamics of linear oscillator coupled to strongly nonlinear attachment with multiple states of equilibrium. Chaos Solitons Fractals **24**(2), 501–509 (2005)
8. Gendelman, O., Gourdon, E., Lamarque, C.-H.: Quasiperiodic energy pumping in coupled oscillators under periodic forcing. J. Sound Vib. **294**, 651–662 (2006)
9. Musienko, A., Lamarque, C.-H., Manevitch, L.: Design of mechanical energy pumping devices. J. Vib. Control **12**(4), 355–371 (2006)
10. Manevitch, L., Gourdon, E., Lamarque, C.-H.: Parameters optimization for energy pumping in strongly nonhomogeneous 2 dof system. Chaos Solitons Fractals **31**(4), 900–911 (2007)
11. Manevitch, L., Musienko, A., Lamarque, C.-H.: New analytical approach to energy pumping problem in strongly nonhomogeneous 2 dof systems. Meccanica **42**(1), 77–83 (2007)
12. Vakakis, A.F., Gendelman, O., Bergman, L., McFarland, D., Kerschen, G., Lee, Y.: Nonlinear Targeted Energy Transfer in Mechanical and Structural Systems I. Springer, Berlin (2009)
13. Vakakis, A.F., Gendelman, O., Bergman, L., McFarland, D., Kerschen, G., Lee, Y.: Nonlinear Targeted Energy Transfer in Mechanical and Structural Systems II. Springer, Berlin (2009)
14. Vakakis, A.F., Manevitch, L.I., Mikhlin, Y.V., Pilipchuk, V.N., Zevin, A.A.: Normal Modes and Localization in Nonlinear Systems. Wiley, New York (1996)
15. Manevitch, L., Gourdon, E., Lamarque, C.-H.: Towards the design of an optimal energetic sink in a strongly inhomogeneous two-degree-of-freedom system. ASME J. Appl. Mech. **74**, 1078–1086 (2007)
16. Schmidt, F., Lamarque, C.-H.: Energy pumping for mechanical systems involving non-smooth saint-venant terms. Int. J. Non-Linear Mech. **45**(9), 866–875 (2010)
17. Manevitch, L., Manevitch, E.: Limiting phase trajectories (LPT) and resonance in a strongly asymmetric 2 dof system. In: Proceedings of 10th Conference on Dynamical System-Theory and Applications, December 7–10, Lodz, Poland (2009)
18. Pham, T., Lamarque, C.-H., Pernot, S.: Passive control of one degree of freedom nonlinear quadratic oscillator under combination resonance. Commun. Nonlinear Sci. Numer. Simul. **16**(5), 2275–2288 (2011). In: Biological and Mechanical Systems in Modern Control Theory, DSTA2009 Conference
19. Farland, D., Bergman, L., Vakakis, A.: Experimental study of non-linear energy pumping occurring at a single fast frequency. Int. J. Non-Linear Mech. **40**(6), 891–899 (2005)

20. Gourdon, E., Alexander, N., Taylor, C., Lamarque, C.-H., Pernot, S.: Nonlinear energy pumping under transient forcing with strongly nonlinear coupling: Theoretical and experimental results. J. Sound Vib. **300**(3–5), 522–551 (2007)
21. Gourdon, E., Lamarque, C.-H., Pernot, S.: Contribution to efficiency of irreversible passive energy pumping with a strong nonlinear attachment. Nonlinear Dyn. **50**(4), 793–808 (2007)
22. Manevitch, L.: Complex Representation of Dynamics of Coupled Oscillators, pp. 269–300. Kluwer Academic/Plenum Publishers, New York (1999)
23. Nayfeh, A.H., Mook, D.T.: Nonlinear Oscillations. Wiley, New York (1979)
24. Gendelman, O., Starosvetsky, Y., Feldman, M.: Attractors of harmonically forced linear oscillator with attached nonlinear energy sink 1: Description of response regimes. Nonlinear Dyn. **51**(1–2), 31–46 (2008)
25. Nguyen, T.: Etude du comportement dynamique et optimisation d'absorbeurs non-lineaires: theorie et experience. Ph.D. thesis, No. order 2010-03, Universite de Lyon, Lyon, France (2010)